Applied Energy 184 (2016) 413–426

Contents lists available at ScienceDirect

Applied Energy

journal homepage: www.elsevier.com/locate/apenergy

Evaluation of uncertainty in the well-to-tank and combustion greenhouse gas emissions of various transportation fuels

Giovanni Di Lullo, Hao Zhang, Amit Kumar *

Department of Mechanical Engineering, 10-263 Donadeo Innovation Centre for Engineering, University of Alberta, Edmonton, Alberta T6G 1H9, Canada

HIGHLIGHTS

- A Monte Carlo simulation is used to quantify uncertainty in the WTT + C emissions.
- Gasoline WTT + C emissions ranged from 95.3 to 138.5 gCO_2 eq/MJ.
- Saudi Arabia crude had the lowest emissions at 95.3–99.9 gCO_2 eq/MJ.
- Venezuela crude had the highest emissions at 113.6–138.5 gCO_2 eq/MJ.
- The largest source of uncertainty is the venting, fugitive, and flaring gas volumes.

ARTICLE INFO

Article history:
Received 27 July 2016
Received in revised form 6 October 2016
Accepted 8 October 2016

Keywords:
Life cycle assessment
Conventional crude
GHG emissions
Transportation fuel
Monte Carlo simulation
Uncertainty analysis

ABSTRACT

Growing concern over climate change has created pressure on the oil and gas industry to reduce their greenhouse gas emissions (GHG). There have been multiple well-to-tank + combustion (WTT + C) studies that have examined various crude oils in an attempt to determine their GHG emission intensities. The majority of these studies published deterministic point estimates with a limited sensitivity analysis. Due to the variation in results between studies and the lack of uncertainty analysis the usefulness of these studies to policy makers and industry representatives is limited. The goal of this study is to expand on the previous literature by identifying a range of WTT + C emissions for crude oils from Saudi Arabia, Venezuela, and Iran. First, the previously published **FUN**damental E**N**gineering Princip**l**E**s**-based Mode**L** for Estimation of **G**reen**H**ouse **G**ases in **C**onventional **C**rude **O**ils (FUNNEL-GHG-CCO) was used to perform a WTT + C analysis of the crudes GHG emissions. Then a Monte Carlo simulation was carried out using existing literature to define input distributions for the key inputs. The resulting gasoline WTT + C GHG emission ranges are 113.6–138.5 (Venezuela High Steam), 101.6–109.9 (Venezuela Low Steam), 101.1–109.2 (Sirri, Iran), and 95.3–99.9 gCO_2eq/MJ (Saudi Arabia). This result indicates that even when uncertainty is taken into account the Venezuelan high steam crude clearly has higher emissions than the Saudi Arabia crude. The results of this study will give policy makers and industry representatives a better understanding of how the WTT + C GHG emissions vary between various crude oils.

1. Introduction

Growing awareness of climate change and global pushes for carbon taxes have led to increased interest in reducing global greenhouse gas (GHG) emissions [1]. Because transportation emissions are responsible for 23% of the global CO_2 emissions, governments have set strategic carbon emission reduction targets. For example, the European Union and California Air Resource Board

Abbreviations: °API, American Petroleum Institute gravity; ANS, Alaska North Slope; CSS, cyclic steam simulation; EF, emission factor (gCO_2/MJ); F-1, original FUNNEL-GHG-CCO model; F-2, modified FUNNEL-GHG-CCO model published by Di Lullo et al.; F-3, modified FUNNEL-GHG-CCO model created for this study; FUNNEL-GHG-CCO, **FUN**damental **EN**gineering Princip**l**E**s**-based Mode**L** for Estimation of **G**reen**H**ouse **G**ases in **C**onventional **C**rude **O**ils; GHG, greenhouse gas; GOR, gas to oil ratio (m^3/m^3); GREET, Greenhouse Gases, Regulated Emissions, and Energy Use in Transportation; GWP, global warming potential; HS, high steam; KYO, know you oil; LCA, life cycle assessment; LHV, lower heating value (MJ/kg); LS, low steam; MD, marine diesel; NG, natural gas; OPGEE, oil production greenhouse gas emissions estimator; OTSG, once through steam generator; P#, #th percentile; P5, 5th percentile; P95, 95th percentile; PG, produced gas; PRELIM, petroleum refinery life cycle inventory model; SF, steam flood; SOR, steam to oil ratio (cold water equivalent m^3/m^3); SP, surface processing; TTW, tank-to-wheel (combustion); ULCC, ultra-large crude carrier; VFF, venting, flaring and fugitive; VLCC, very large crude carrier; WAG, water-alternatin-gas; WF, water Flood; WOR, water-to-oil ratio (m^3/m^3); WTR, well-to-refinery gate; WTT, well-to-tank; WTT+C, well-to-tank + combustion.

* Corresponding author.
E-mail address: amit.kumar@ualberta.ca (A. Kumar).

http://dx.doi.org/10.1016/j.apenergy.2016.10.027
0306-2619/

have implemented polices to reduce the carbon intensity of transportation fuels by 6% and 10%, respectively, before 2020 [2,3]. One solution to meet these targets is to consume transportation fuels (gasoline, diesel and jet) with lower upstream emissions.

The upstream emissions from transportation fuels are generated during crude oil extraction, surface processing, transportation, refining, and distribution. Life cycle assessments (LCAs) have been used to quantify emission intensity (emissions produced per unit of product produced) by examining the energy used and emissions generated along the life cycle stages from extraction of natural resources to the end of the product life [4]. The upstream emissions from different crudes will vary depending on the crude properties and the methods used to extract and process the crudes into finished transportation fuels.

A well-to-tank + combustion (WTT + C) analysis is a specific type of LCA which focuses on the transportation fuel only and ignores the emissions associated with vehicle production, maintenance and disposal. As the emissions released from one megajoule of fuel will not vary from vehicle to vehicle a WTT + C analysis of multiple crudes can be used to compare the crude GHG emission intensities. A full LCA including the vehicle would be more appropriate for comparing internal combustion engine emission intensities to hydrogen fuel cell and battery electric vehicles using a regional average gasoline emission intensity. This study is focused on comparing specific transportation fuel production pathways not regional averages.

Current literature examines WTT + C emissions of transportation fuels, which includes the upstream to combustion emissions, through models. These models can be divided into two types. Type 1 models, such as Greenhouse Gases, Regulated Emissions, and Energy Use in Transportation (GREET) [5], GHGenius [6], and Orsi et al. [7] use a top-down approach in which high level aggregated facility- and country -level data are used to calculate industry average emissions. However, the use of aggregated data makes it difficult to determine emission intensity for specific crudes. Type 2 models, such as Jacobs [8,9], TIAX [10], Oil Production Greenhouse gas Emissions Estimator (OPGEE) [11], Petroleum Refinery Life Cycle Inventory Model (PRELIM) [12], and **FUN**damental **EN**gineering Princip**l****E**s-based Mode**L** for Estimation of **G**reen**H**ouse **G**ases in **C**onventional **C**rude **O**ils (FUNNEL-GHG-CCO) [13–16], use a bottom-up approach wherein energy consumed and emissions generated are calculated using engineering first principles for each stage. Due to the lack of information and process complexity, the bottom-up models only examine processes that consume or produce large amounts of energy or pollution, and so they do not capture all the emissions produced and may lead to modeling results with limited accuracy. However, a bottom-up model can calculate the emissions for specific crudes and provide detailed results for each sub-process.

Various bottom-up models have determined the WTT + C emissions for over 35 crudes; however, the results are difficult to compare due to differences in the boundaries and assumptions used. Additionally, the TIAX and Jacobs models lack transparency and reproducibility as they were conducted by consulting companies and used confidential data [8–10]. Gordon et al.'s report "Know Your Oil" (KYO) used the PRELIM and OPGEE models to develop WTT + C estimates for thirty crude oils using consistent boundaries [17]. However, all these models provide deterministic point estimates for the WTT + C emissions. Without an uncertainty analysis, it is not possible to accurately compare crudes based on their WTT + C emissions. If model uncertainty is high compared to the difference in the emissions between two crudes, it would not be accurate to claim that one crude has lower emissions than the other. Di Lullo et al. examined the uncertainties in five North American crudes using a updated version of the FUNNEL-GHG-CCO model and found that the uncertainties in the WTT + C emissions ranged from ±2.6 to ±10.4% [16]. Although the uncertainty ranges could be large it was still possible to differentiate between the highest and lowest emitting crudes [16]. This work also looks to examine specific crude production pathways rather than regional averages. While regional averages are beneficial for high level policy decisions and examination of specific pathways allows a more detailed comparison of various technologies. Future work will compare these results to oil sand pathways as well as alternative technology pathways.

There are three main gaps in the previously published work. First, the Jacobs [8,9] and TIAX [10]models lack transparency, and reproducibility. Second, the published literature only examines uncertainty in 5 out of the 35 crudes studied. Both gaps are important to policy makers and industry representatives because quantifying the uncertainty in WTT + C emissions will provide a more accurate representation of the industry.

The general objective of this study is to determine the WTT + C emission uncertainties for Saudi Arabia, Iran, and Venezuela oils. The specific objectives are to:

1. Conduct a transparent and reproducible WTT + C analysis of crude oils from Saudi Arabia, Iran, and Venezuela previously examined by Jacobs and TIAX with the FUNNEL-GHG-CCO model.
2. Determine the WTT + C emission uncertainty by performing a Monte Carlo simulation using a range of values from multiple data sources.

The remaining 27 crudes are not examined as it is difficult to find sufficient data due to the depth of the analysis. To limit the scope to a reasonable size and align with previous literature only U.S. refineries are examined. The Saudi Arabia and Venezuela crudes were chosen as they represent 17% and 11% the crude imported to the USA from 2011 to 2015 [18], a significant portion of the USA's imports. While the USA does not currently import any Iranian oil, this oil was included due to the potential for imports as a result of the lifting of the Iranian trade embargo in 2016 [18,19].

The uncertainty ranges determined from this study will provide a fair representation of the industry and a GHG emission comparison among the three crude oils. The results will help policy makers understand the limitations of WTT + C models and will help identify data gaps from industry in order to improve the accuracy of the WTT + C GHG emission estimates.

2. Methodology

This study was conducted in two stages. In the first stage we performed a WTT + C analysis for crude oils from Saudi Arabia, Iran, and Venezuela. Data were collected and fed into a modified version of the FUNNEL-GHG-CCO model to complete the WTT + C analysis. The scope of this WTT + C model comprises of site preparation, extraction, surface processing, crude transportation, refining, distribution, and combustion stages. The study's second stage was an uncertainty analysis on the WTT + C emissions. First, a sensitivity analysis was used to identify sensitive inputs that would have a significant effect on the results. Uncertainty distributions were then determined for the sensitive inputs and were used in a Monte Carlo simulation to determine the uncertainty. The Monte Carlo simulations are run using ModelRisk which is a Microsoft Excel add-in [20].

2.1. Base case model

The original FUNNEL-GHG-CCO model was created by Rahman et al. in 2014 and uses engineering first principles to perform a

bottom-up analysis [13–15]. This model was used to study five conventional North American crudes (Maya, Mars, Bow River, Alaska North Slope, and California Kern) and determine deterministic point estimates for the WTT + C emissions of each crude. The crudes were extracted using water flooding, nitrogen gas injection, water-alternating-gas (WAG) injection, and steam injection. The FUNNEL-GHG-CCO model focuses on crudes refined and used within the USA. Further work by Di Lullo et al. [16] modified the existing FUNNEL-GHG-CCO model to increase its accuracy and performed an uncertainty analysis to determine probable ranges for the five conventional crude oils. Details on the original and modified FUNNEL-GHG models can be found in earlier work [13–16].

The FUNNEL-GHG-CCO model uses a functional unit of gCO_2eq/MJ of gasoline/diesel/jet fuel. This article focuses on gasoline production; diesel and jet fuel production emissions are included in Supplementary Information (SI) Section S4. Fig. 1 gives a high level overview of the seven main stages.

The model used by Di Lullo et al. [16] will be referred to as the F-2 model, and the original FUNNEL-GHG-CCO model will be referred to as the F-1 model. This study made four additional modifications to the F-2 model to accommodate the new crudes and provide additional accuracy improvements; the model used in this paper is referred to as the F-3 model.

The modifications to the F-3 model are these: first, the F-1 and F-2 models used values (emission factors [EFs] and energy densities) from the 2013 version of GREET while the F-3 model uses the 2015 version of GREET. Second, the electricity emission factors have been updated to use consistent boundaries. Earlier versions did not include upstream EFs for the regional grid emission factors. Third, the water treatment in the original and F-2 model assumed that injected water would use treated produced water first and only import sea water if there was insufficient produced water available. The F-3 model allows the user to specify whether the produced water is reused or if all the injected water is imported. Fourth, this model updated the distributions used for the crude transportation stage to improve accuracy. Further details on the modified electricity EFs and crude transportation distributions are in Section S3 of the SI.

2.2. Overview of new crude oils

Crude oil properties vary significantly around the world and are classified by their American Petroleum Institute gravity (°API) as light (>31.1 °API), medium (22.3–31.1 °API), heavy (10–22.3 °API), and extra-heavy (<10 °API). The API gravity is related to the inverse of the crude's density with water being 10°API [21]. This study performs a WTT + C analysis on light crudes from Saudi Arabia, heavy crude from Venezuela, and medium crude from Iran. The Saudi Arabia and Venezuela crudes were chosen as they represent a significant portion of the USA's imports. Iranian oil was included due to the potential for imports as a result of the lifting of the Iranian trade embargo in 2016 [18,19]. Additionally, earlier studies on these crudes lacks transparency with respect to data inputs, and do not incorporate an uncertainty analysis [8–10]. Table 1 shows a summary of the crude oils.

2.2.1. Saudi Arabia

The Gwahar oil field is over 2000 square miles and is split into multiple zones. The Ain Dar and Uthmaniyah zones both extract oil from the Arab-D formation and produce a majority of the field's oil [22,23]. As a result, this study focuses on Saudi Arabian light crude (Arab Light) from the Arab-D formation. The crude from the northern Ain Dar zone has an API of 34° [24], and the crude from the lower Uthmaniyah zone has an API of 32.6° [22]. The entire Gwahar field produced approximately 5 million bpd in 2003 [23]. The field currently uses water injection to maintain reservoir pressure. The extracted oil is gathered at Abqaiq for surface processing [23]. The stabilized crude is then transported through the 1200 km Petroline to the Yanbu terminal, where it is loaded onto very large crude carriers (VLCC) and ultra-large crude carriers (ULCC) for transport to the USA [25].

2.2.2. Venezuela

Bachaquero crude is produced in the Bolivar oilfield on the east coast of Lake Maracaibo [26]. The heaviest cut of Bachaquero crude was used to align with the Jacobs study and has an API of 11.7° [8,27]. Steam flooding (SF) and cyclic steam simulation (CSS) are used to extract the heavy crude using offshore platforms [26–30]. It is assumed that the crude is then transported via pipeline to the Gulf of Venezuela coast where it is loaded onto a crude tanker.

2.2.3. Iran

The Alvand, Nosrat, Sivand, and Dena oilfields are located off the coast of Sirri Island in the Persian Gulf [31,32]. Water injection is used to produce medium 31° API oil from offshore platforms [33]. This study focuses on the Sirri C&D fields due to data availability. The crude undergoes surface treatment on Sirri Island and

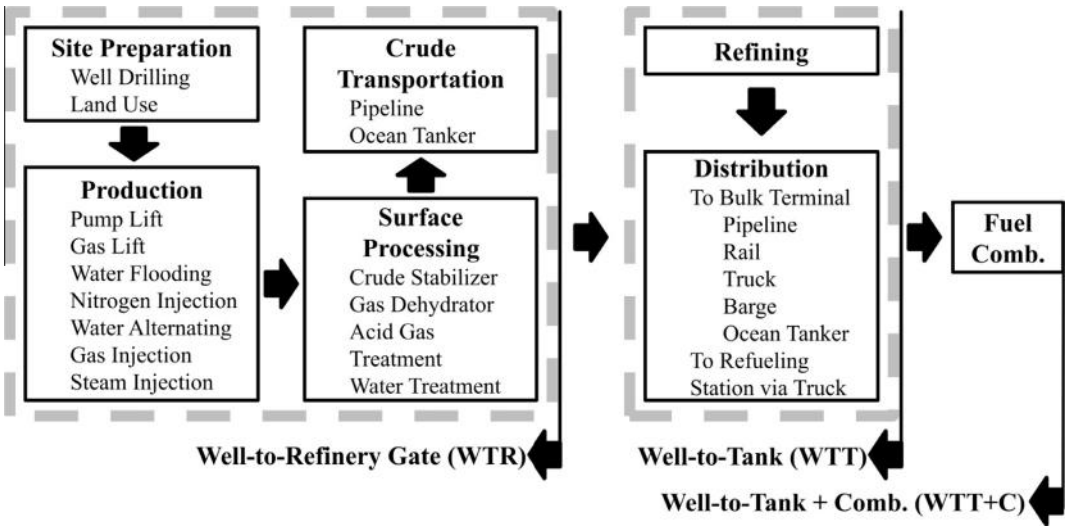

Fig. 1. FUNNEL-GHG-CCO model boundary.

Table 1
Summary of crude oil fields.

Crude name	°API	Country	Field	Extraction technique
Arab Light	32.6	Saudi Arabia	Arab-D section of the Gwahar field	Water flooding
Vene	11.7	Venezuela	Bachequero-13	Steam flooding and cyclic steam simulation
Sirri	31	Iran	Sirri C&D	Water flooding

is then loaded onto ultra-large crude carriers(ULCC) moored offshore [31,34].

3. Life cycle assessment of WTT + C greenhouse gas emissions

This section covers the WTT + C analysis of the study. Each life cycle stage is described, followed by the WTT + C results.

3.1. Goal and scope definition

As described in Section 2, this study examines the WTT + C emissions of transportation fuel production. A bottom-up analysis is used to quantify the energy and mass balances for each life cycle stage. A functional unit of gCO_2eq/MJ crude is used for pre-refinery emissions and gCO_2eq/MJ gasoline/diesel/jet fuel for the WTT + C emissions.

3.2. Life cycle inventory

This section provides the inputs used for the WTT + C analysis of the new scenarios. Only a high level description of the calculations used is given in this study; for additional details on the calculations readers are encouraged to read the previous works from Rahman et al. and Di Lullo et al. [13–16].

3.2.1. Site preparation

Site preparation emissions are those from well drilling and land alteration. Diesel fuel used to run the drill is the primary pollution source [11,13]. The amount of drilling emissions is dependent on the drilling depth and the well lifetime productivity (as shown in Table 2). The lifetime well productivity is approximated from the total oil recovered and the number of wells drilled [35].

The land use emissions are a result of carbon from the soil and biomass being oxidized during well construction and from the land's reduced ability to sequester carbon after being disrupted [36,37]. The land use emissions depend on the carbon richness of the ecosystem and the drilling intensity [36]. Since Sirri and Venezuela production occurs offshore and Saudi Arabia is a desert, low carbon richness was assumed for all three crudes. A moderate drilling intensity was assumed for all scenarios. The land use emissions were taken from OPGEE using a 30 year time period [11].

3.2.2. Extraction and surface processing

The extraction and surface processing emissions are primarily dependent on the injection and production steam-to-oil (SOR), water-to-oil (WOR), and gas-to-oil (GOR) ratios (shown in Table 3). The Venezuela SF and CSS extraction emissions are calculated from the amount of steam required and the energy required to heat the steam. The Venezuelan base case assumes 1924 kJ/kg of energy are required to produce the 75% quality steam required for injection [27,40]. Steam energy calculations are provided in Section S2.2 of the SI. Due to the wide range of SORs found in the literature, both a high steam (HS) scenario and a low steam (LS) scenario are used for the Venezuelan crude; the only difference between the two scenarios is the steam injection ratio, as seen in Table 3. Sirri and Arab Light water flooding (WF) extraction emissions are calculated from the amount of energy required for the injection pump. An injection pump discharge pressure of 27.6 and 20.7 MPa is used for the Sirri and Arab Light scenarios based on their reservoir pressures [33,41,42]; additional detail is in Section S2 of the SI.

The surface processing stage uses the same calculations as those in the F-1 and F-2 models [13–16]. There are no crude-specific inputs other than the water injection and production ratios. The Sirri scenario is unique as the produced water is not reinjected but disposed of into the ocean [43], resulting in a larger volume of water requiring treatment. Further details are given in Section S2.3 of the SI.

Table 2
Drilling stage inputs.

Crude	Vene	Sirri	Arab Light
Average depth (m)	914 [27]	2438 [33]	2042 [23]
Well lifetime productivity (m^3/well)	537,021[a]	364,876[b]	36,567[c]

[a] Approximated from initial oil-in-place of 7.04e9 bbl, 300 wells and 14.4% oil recovery factor [27].
[b] Approximated from initial oil-in-place of 27e6 bbl, 2 wells and 17% oil recovery factor [33].
[c] Approximated from 345e6 bbl 2008 cumulative production and active 1500 wells [38,39].

3.2.3. Venting, fugitive, and flaring emissions

During the crude extraction, surface processing, transportation, and refining stages, hydrocarbon gas is either vented or leaks into the atmosphere; this gas is known as venting and fugitive emissions. The F-2 model used previous work by Canter et al. [44] that calculated the venting and fugitive gas volumes as a percentage of the produced gas volume for North American crudes. As there is no additional information available for crudes outside of North America, the same percentage of 4.6% is used for this study [16].

Flaring emissions occur when the produced gas (PG) is combusted as it is vented to the atmosphere. The flaring rate is calculated from the respective countries' annual flaring and oil production volumes and results in flaring rates of 6.5, 14.8, and 46.5 m^3 PG/m^3 crude for the Arab Light, Vene, and Sirri scenarios, respectively. Further details are provided in Section S3.1 of the SI.

The produced gas composition is used to determine the EF for the vented, fugitive, and flared (VFF) gas. All crudes except for Arab Light use the default gas composition from the F-1 and F-2 models, which is derived from OPGEE due to lack of data [11,13,16]. The Arab Light scenario uses crude-specific gas composition from the northern Ain Dar field, which has a lower methane concentration (44.3 vs. 84.0 mol%) [42]. The full gas composition is provided in Table S2 in the SI.

The F-2 model introduced a produced gas credit [16]. The credit is defined as the natural gas extraction and processing emissions, as the produced gas can be used to offset the natural gas consumption. This model assumes all produced gas that is not reinjected or lost is sold as produced gas.

3.2.4. Crude transportation

The crudes are transported from the extraction and surface processing sites to the refinery in three stages. First, the crude is transported from the surface processing site to the coast via pipeline, then it is transported to the USA via tanker, and finally it is trans-

Table 3
Injection and production ratios.

Crude	Extraction technology	Inj. WOR (m^3/m^3)	Inj. SOR (m^3/m^3)	Prod. WOR (m^3/m^3)	Prod. GOR (m^3/m^3)
Vene low steam	Steam flooding and cyclic steam simulation	N/A	0.25	2.0	98.0
Vene high steam	Steam flooding and cyclic steam simulation	N/A	2.10	0.3	98.0
Sirri	Water flooding	2.7	N/A	1.0	133.6
Arab Light	Water flooding	1.8	N/A	0.7	101.5

ported inland to the refineries via pipeline. It is assumed that all three crudes are refined in Houston, as 98% and 65% of Venezuelan and Persian Gulf crude are imported to PADD 3 [45].

The pipeline calculations are unchanged from the F-2 version and use scenario-specific inputs (provided in Table 4) to calculate the pumping energy required to overcome frictional losses. Additional information on how the pipeline velocities and throughputs are determined is in Section S3.2 of the SI.

Using the GREET calculation method, we approximated the marine tanker emissions from the tanker capacity, travel distance, velocity, and load factors [5]. The tanker capacity is determined from the origin port limitations, and the distances between the ports are determined from Sea-Distance-org; both are shown in Table 5 [5]. The load factors refer to the average engine load, the delivery trip uses a load factor of 0.83, and the return trip uses 0.70 [5]. The tanker velocity is assumed to be 15 knots for all scenarios [5].

3.2.5. Refining

The refinery emissions are calculated using the Aspen HYSYS model previously used in the F-1 and F-2 models. The crude assays for Arab Light [51], Venezuela Bachaquero Heavy [56], and Sirri offshore [50] were input to the Aspen model to determine the refinery emissions and refinery yield factor. Mass-based allocation was used to track the emissions through the refinery to determine each product's share of the refinery emissions. The refinery yield factor is used to convert pre-refinery emissions from gCO_2eq/MJ crude to gCO_2eq/MJ gasoline/diesel/jet. It represents the inverse of the refinery conversion efficiency. If the refinery yield factor is 1.25, then 1.25 MJ of crude is required to produce 1 MJ of desired products, where gasoline, diesel, and jet fuel are the desired products. The remaining 0.25 MJ is either lost or converted to undesirable products such as coke or heavy fuel oils. The pre-refinery emissions are multiplied by the refinery yield since more than 1 MJ of crude must be extracted and transported to the refinery to produce 1 MJ of desired end product.

3.2.6. Distribution and vehicle combustion

The final products are distributed from the refinery to bulk terminals using a combination of ocean tankers, barges, pipelines, and trucks. Trucks are then used to distribute the products from the bulk terminals to the fueling stations. As all the crudes examined are refined in North America there is no variation in the distribution and combustion emissions between scenarios. Since the fuel properties will be identical for each crude the vehicle driving cycles are ignored as they would introduce unnecessary uncertainty and will not affect the crude comparison.

Table 5
Crude marine tanker transportation data.

Crude	Origin	Distance (km) [53]	Capacity (DWT)
Vene	Maracaibo City	3408	240,000[a]
Sirri	Sirri Island	22,561	240,000[a]
Arab Light	Yanbu	22,743	315,000[b]

[a] Typical VLCC and ULCC vary from 160,000 to 330,000 DWT; this research used the average as the default [34,54].
[b] Typical tankers range from 280,000 to 350,000 DWT; this research used the average as the default [55].

3.3. WTT + C analysis emission factors

This section provides the key EFs used in the analysis; full details on how the EFs are calculated from the reference values are provided in Section S3 of the SI. The NG Upstream EF is the only Fuel EF in Table 6 not taken directly from GREET; it is determined from work by Weber et al. [57] that examined uncertainty in NG upstream emissions. The marine residual oil LHV is 39.5 MJ/kg [5]. Electricity EFs are calculated using GREET values and regional electricity grid mixes [5]. The fuel upstream emissions and 6.5% transmission losses are included in the values provided in Table 7. The final product distribution EFs are taken from GREET and vary for each product as shown in Table 8. Vehicle combustion EFs, also from GREET, are 73.3, 75.9, and 72.9 gCO_2eq/MJ for gasoline, diesel, and jet fuel, respectively [5].

3.4. WTT + C analysis results

The WTT + C analysis found that the heavy Venezuelan crudes had the highest emissions and Arab Light the lowest (shown in Fig. 2). This is expected, as the heavier crude requires a more energy intensive extraction and refining process. The difference in emissions between the gasoline, diesel, and jet fuels is a result of the different refinery, distribution, and combustion emissions for each product; the pre-refinery emissions (WTR) are the identical for gasoline, diesel, and jet fuel.

Table 4
Crude pipeline transportation data.

Crude	Origin	Destination	Distance (km)	Velocity (m/s) [46–48]	Throughput (m^3/d) [47]	Kinematic viscosity (cSt)
Vene	Bachaquero	Gulf of Venezuela	125[a]	1.4	63,500	48.6 [49]
Sirri	Platform	Sirri Island	50[b]	3.3	63,500	20.3 [50]
Arab Light	Abqaiq	Yanbu	1200[c]	3.3	476,962	10 [51,52]
USA	Houston port	Houston refineries	80[d]	1.4/2[e]	63,500	Crude specific

[a] Google map's distance from Bachaquero to coast.
[b] Farthest field from Sirri Island [32].
[c] Length of the Petroline [48].
[d] From F-1 model, approximate distance from port to refineries [13–15].
[e] 1.4 m/s for Vene, 2 m/s for Sirri and Arab Light [46–48].

Table 6
Fuel emission factors [5] (gCO_2eq/MJ).

Emission source	Value
Stationary diesel engine comb.	73.43
Industrial natural gas boiler comb.	56.52
Natural gas turbine comb.	56.32
Diesel upstream	15.74
Natural gas upstream [57]	17.96
Produced gas credit	12.52
Marine residual oil comb.	80.84
Marine diesel upstream	12.75

Table 7
Electricity emission factors ($gCO_2eq/kW\,h$).

Electricity use	EF	Sources
Vene extraction & pipeline 1[a]	531	[58,59]
Sirri extraction & pipeline 1[a]	877	[60]
Saudi Arabia extraction	869	[61,62]
Saudi Arabia pipeline 1	767	[63]
Pipeline 2[b] & Houston refinery	656	[64]

[a] Pipeline 1 carries crude from the extraction site to the origin marine port.
[b] Pipeline 2 carries crude from destination marine port to the refinery.

Table 8
Final product distribution to end user EF [5] (gCO_2eq/MJ).

Method	Gasoline	Diesel	Jet
Ocean tanker	0.544	0.262	0.260
Barge	0.623	0.372	0.369
Pipeline	0.240	0.208	0.206
Rail	0.100	0.330	0.325
Truck	0.140	0.142	0.141

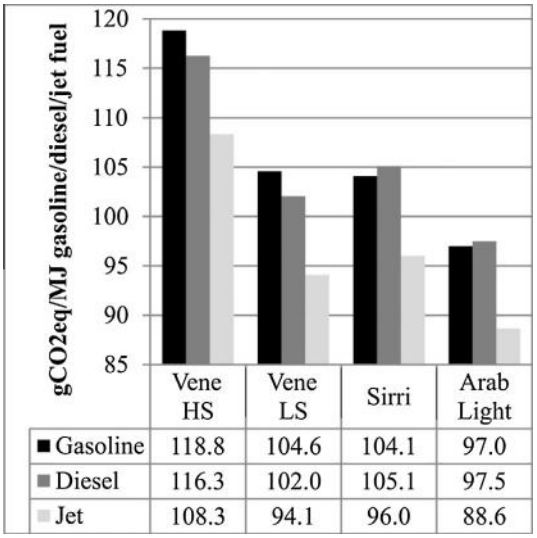

Fig. 2. Well-to-tank + combustion emissions.

3.4.1. Well-to-refinery gate results

Fig. 3 shows the breakdown of well-to-refinery gate (WTR) emissions for gasoline, diesel, and jet fuel production. The results show that the extraction, VFF, and crude transportation stages are the primary emissions sources. All emissions are shown in terms of gCO_2eq/MJ of crude for pre-refinery emissions and are identical for all three fuels. The site preparation emissions range from 0.13 to 0.21 gCO_2eq/MJ for Vene and Arab Light, respectively. The land-use emissions are 0.13 gCO_2eq/MJ for all four scenarios and contribute to the majority of the site preparation emissions.

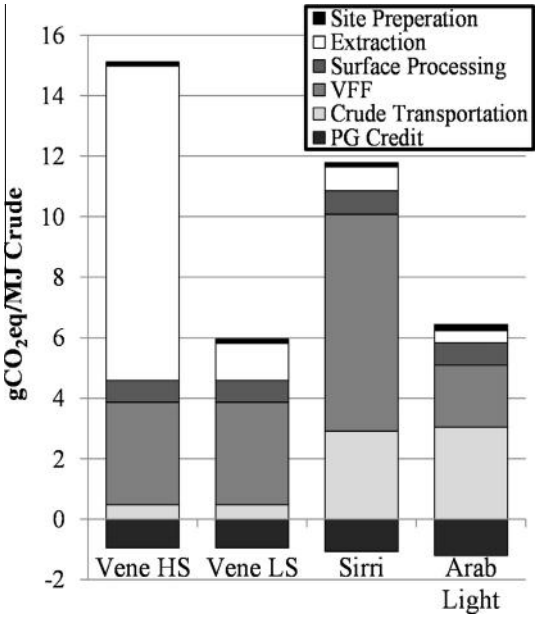

Fig. 3. Well-to-refinery gate emissions.

The drilling emissions for Vene are negligible due to the high well lifetime productivity. The extraction emissions are from steam generation for the Vene scenarios and water injection for the Sirri and Arab Light scenarios. The Sirri emissions are higher than the Arab Light emissions because of the higher water injection ratio and injection pressure used. The Vene scenarios have the highest emissions as the thermal extraction method is more energy intensive. The surface processing emissions range from 0.72 to 0.78 gCO_2eq/MJ for Vene and Sirri, respectively; the crude oil stabilizer contributes to 85–91% of the surface treatment emissions. Sirri has the highest VFF emissions due to its high gas-to-oil ratio (GOR) and large flaring volumes (see Table 9). Arab Light has the lowest VFF emissions because its produced gas has a low methane concentration and a low flaring rate. Even though the Sirri scenario has a larger GOR, the Arab Light scenario has a larger gas credit because Sirri flared a larger portion of its produced gas. The crude transportation emissions are low, 0.48 gCO_2eq/MJ for Vene, as the marine transportation distance is shorter (3400 versus 23,000 km for Sirri and Arab Light). Table 10 provides a breakdown of the crude transportation emissions. The pipeline emissions were small due to the relatively short transportation distances.

3.4.2. Refinery, distribution, and combustion emissions

Refinery emissions vary for each crude and final product (see Table 11) Jet fuel is made of the light ends of the crude feedstock that go through mild treatment and as a result have the lowest emissions. For the lighter crudes, Sirri and Arab Light, the diesel emissions are higher than the gasoline emissions, while for the heavy crude the opposite is true; this is a result of the crude composition and refinery configuration. The refinery yield factors are 1.55, 1.33, and 1.25 for the Vene, Sirri, and Arab Light scenarios, respectively. The Vene scenario has the highest yield factor because it is a heavier crude and will produce larger amounts of undesirable products such as residual oil. The pre-refinery emissions in gCO_2eq/MJ crude are multiplied by the refinery yield factor to get emissions in gCO_2eq/MJ gasoline/diesel/jet fuel. Since all the crudes are refined and distributed in North America, distribution and combustion emissions are the same for all the crudes. Distribution emissions for gasoline, diesel, and jet fuel are 0.50, 0.44, and 0.43 gCO_2eq/MJ and combustion emissions are 73.27, 75.86, and

Table 9
VFF and PG credit emissions (gCO_2eq/MJ crude).

Crude	Vene HS	Vene LS	Sirri	Arab Light
Venting and fugitive	2.28	2.28	3.37	1.39
Flaring	1.11	1.11	3.80	0.66
% Flaring	32.8%	32.8%	53.0%	32.1%
PG credit	−0.95	−0.95	−1.07	−1.20

Table 10
Crude transportation emissions breakdown (gCO_2eq/MJ crude).

Crude	Vene HS	Vene LS	Sirri	Arab Light
Pipeline 1[a]	0.02	0.02	0.07	0.38
Marine	0.45	0.45	2.82	2.65
Pipeline 2[b]	0.01	0.01	0.01	0.02
Total	0.48	0.48	2.90	3.05

[a] Pipeline 1 carries crude from the extraction site to the origin marine port.
[b] Pipeline 2 carries crude from destination marine port to the refinery.

Table 11
Refinery emissions by product fuel (gCO_2eq/MJ gasoline/diesel/jet).

Crude	Gasoline	Diesel	Jet
Vene	23.03	16.50	11.50
Sirri	16.06	13.12	7.02
Arab Light	16.68	13.15	7.26

72.89 gCO_2eq/MJ. The combustion emissions represent 61–82% of the total WTT + C emissions.

4. Uncertainty analysis of WTT + C emissions

This section covers the method and results of the uncertainty analysis. Only an overview is provided here; detailed technical information can be found in the SI. The uncertainty analysis uses a functional unit of gCO_2eq/MJ gasoline/diesel/jet fuel. Only a breakdown of the gasoline WTT + C emissions is provided in the main report as the diesel and jet fuel results are very similar. The diesel and jet fuel results are in Section S4 of the SI.

4.1. Uncertainty analysis methods

The uncertainty in the model output is due to sensitivity and uncertainty in the model inputs. Hence, a sensitivity analysis was used to identify sensitive inputs. Distributions were then generated for each of the sensitive inputs from the available literature. Finally, a Monte Carlo simulation was used to quantify the uncertainty for each scenario.

4.1.1. Sensitivity analysis

Since tank-to-wheel (TTW) emissions are constant across all scenarios they are not included in the sensitivity analysis; instead well-to-tank (WTT) emissions are used. In order for an input to be deemed sensitive, a ±25% change in the input value must result in a change of ±1% or greater in the WTT emissions. A change of ±0.1% to ±1% is considered semi-sensitive and a change of less than ±0.1% is deemed insensitive. Even if an input is deemed insensitive, the output uncertainty could be significant if the input uncertainty is significantly larger than ±25%. Hence in this study, the lists of semi-sensitive and insensitive inputs were reviewed and any inputs that were identified as having large uncertainties were reclassified as sensitive inputs.

4.1.2. Determining distributions for sensitive inputs

In order to create a statistical distribution, a significant amount of data is required. When limited data are available, this study uses triangular distributions that require a most likely, minimum, and maximum estimate to generate. Additionally, triangular distributions are more conservative as they favor extreme values [65]. ModelRisk copulas are used to model dependence between inputs to produce a more conservative result [20,66].

4.1.3. Determining distributions for the insensitive inputs

Even though the insensitive inputs individually have an insignificant effect, they can collectively impact the WTT + C emissions. As a result, the insensitive inputs are assigned a triangular distribution with a minimum and maximum value of 90% and 110% of the base case value. This will give a wider, more conservative output distribution.

4.1.4. Monte Carlo simulation parameters

To ensure the sampling error is less than 0.1 g/MJ, 50,000 samples are used for each scenario. Sampling error calculations are in Section S1 of the SI. Reported results use the 5% and 95% percentiles (P5, P95) to capture the extreme estimates.

ModelRisk tornado plots were used to identify which inputs had the largest contribution to the overall uncertainty. The tornado plots were generated using the conditional mean and 20 tranches. This means that the Monte Carlo samples are divided into 20 subgroups based on the value of the input being examined. For example, subgroup 1 includes all samples where input X's value is in the P0-P5 range of its distribution. The mean of each subgroup is calculated and the tornado plot displays the minimum and maximum subgroup mean. Due to the number of inputs modeled and limited accuracy of the tornado plots, only the significant inputs are displayed. Significant inputs have a tornado plot variance (maximum - minimum) that is greater than 10% of the WTT + C variance (P95-P5). Spider plots were also used to identify any non-linear responses.

This study does not include an in-depth analysis of the uncertainty in the refinery process. The F-1 model uses Aspen HYSYS to model a typical North American refinery and this model is used unchanged in the current work [13–15]. The Aspen model outputs mass and energy balances for each refinery unit and these values are used to allocate emissions to each sub process using mass-based allocation [13–15,67]. In order to determine refinery emissions, the energy balances are multiplied by heater and boiler

efficiencies and fuel EF. This study includes uncertainty ranges for the efficiencies and EFs only and does not consider uncertainty in the mass and energy balances for each process unit. The refinery uncertainty is then fed into the WTT + C model as an input uncertainty to estimate the WTT + C uncertainty.

4.2. Monte Carlo inputs

Tables 12 and 13 show the distributions used for common and crude-specific inputs. Most of the common inputs have been taken unchanged from the F-2 model [16]. The EF ranges were determined using GREET as the most likely value and uncertainty ranges from Weber and Calvin [57]. The electricity EFs were defined using the regional grid electricity mix and GREET defaults. The unit efficiencies, surface processing (SP), and crude transport distributions were determined by examining several references and using judgment to define probable ranges. The venting and fugitive emissions distributions were determined from work by Canter et al. [44]. The flared gas volume distributions used the measurement error specified by the NOAA data [68]. Data from OPGEE and other sources were used to define probable ranges [11] for the flaring efficiency and PG methane concentration. The refinery yield factor range is based on the authors' judgment from reviewing variations in the Aspen model results with various crude assays and work from PRELIM [12,67]. Additional details can be found in Sections S2 and S3 of the SI, and the previously published literature [16].

4.3. Uncertainty analysis results

Only the gasoline emissions are examined in detail here; the diesel and jet fuel tornado plots are in Section S4 of the SI. Fig. 4, shows that even when considering uncertainty the Vene HS scenario clearly has higher WTT + C emissions than the remaining scenarios since there is no overlap in the uncertainty ranges. However, it is not possible to conclude whether the Vene LS or Sirri scenario has higher or lower emissions as their uncertainty ranges have a significant amount of overlap. The Monte Carlo simulation was run twice for each scenario, once with the insensitive input distributions included and once with constant insensitive inputs. The difference between the two results was within sampling error, verifying that the insensitive inputs did not have a significant effect on the final results.

The results for diesel and jet fuel are similar to the gasoline results. Fig. 4 shows that the Sirri WTT + C emissions are higher than the Vene LS WTT + C emissions for diesel and jet fuel while for gasoline the opposite is true. This difference is a result of the refinery configuration and crude composition. The heavier Venezuelan crude requires more energy to produce gasoline compared to the lighter Sirri crude.

4.3.1. Sources of uncertainty in WTT + C emissions

The tornado plots in Fig. 5 identify which input distributions had the largest effect on WTT + C emission uncertainty. The refinery emissions had the largest effect in every scenario except in the

Table 12
Common Monte Carlo input distributions.

	Input	Monte Carlo Distribution	Units	Source
Emission factor	Methane GWP[a]	Triangle (20.74, 34, 47.26)		[69,70]
	NG upstream[a]	Triangle (71.2%, 100%, 140%)		[5,57,71]
	NG boiler comb.[a]	Triangle (97.2%, 100%, 102.7%)		[5,57]
	NG turbine comb.[a]	Triangle (96.9%, 100%, 102.4%)		[5,57]
Electricity EF	Arab Light extraction	Triangle (502, 869, 1200)	$gCO_2eq/kW\,h$	[5,61]
	Arab Light pipeline 1	Triangle (690, 767, 844)	$gCO_2eq/kW\,h$	[5,63]
	Vene extraction & pipeline 1	Triangle (254, 531, 803)	$gCO_2eq/kW\,h$	[5,59]
	Sirri extraction & pipeline 1	Triangle (699, 877, 1105)	$gCO_2eq/kW\,h$	[5,60]
	Pipeline 2 + Houston refinery	Triangle (502, 656, 804)	$gCO_2eq/kW\,h$	[5,64]
Unit Eff.	Boiler[a]	Triangle (62%, 75%, 88%)		[72–75]
	Heater[a]	Triangle (70%, 80%, 90%)		[11,13,76,77]
	Low flow pump[a]	Triangle (50%, 60%, 70%)		[78]
	High flow pump[a]	Triangle (50%, 65%, 85%)		[8,11,14,48,78,79]
	Pipeline pump	Triangle (75%, 85%, 92%)		[48,79–81]
Surface processing	Specific heat correction factor[a]	Triangle (0.84, 1, 1.5)		[82]
	Crude stabilizer inlet temp.[a]	Triangle (37.8, 48.9, 65.6)	°C	[83]
	Crude stabilizer outlet temp.[a]	Triangle (93.3, 173.3, 204.4)	°C	[83,84]
	Produced water energy intensity[a]	Triangle (1.51, 2.26, 5.79)	$kW\,h/m^3$	[13,85]
	Imported water energy intensity[a]	Triangle (1.26, 1.51, 3.90)	$kW\,h/m^3$	[13,85]
Crude transport	Heavy crude pipeline velocities	Triangle(0.8,1.4,2.0)	m/s	[47]
	Light/medium crude pipeline velocities	Triangle (1.3, 2.0, 3.1)	m/s	[47]
	Middle Eastern light crude pipeline velocities	Triangle (2.0, 3.3, 3.8)	m/s	[46–48]
	Pipeline throughput	Triangle (15,900, 63,600, 127,200)	m^3/d	[47]
	Marine distances	Triangle (90%, 100%, 110%)		
	Arab Light ocean tanker capacity	Triangle (280,000, 315,000, 350,000)	DWT	[55]
	Sirri and Vene ocean tanker capacity	Triangle (160,000, 240,000, 320,000)	DWT	[54]
	Tanker velocity	Triangle (22.2, 27.8, 31.5)	km/h	[54,86–88]
	Marine fuel comb. EF	Triangle (95%, 100%, 105%)		[5]
	Residual oil energy density	Triangle (37.7, 39.5, 41.6)	MJ/kg	[5]
VFF and other	Vented & fugitive gas volumes[a]	Triangle (2.1%, 4.6%, 7%)		[44]
	Arab light flared gas volume	Triangle (2.16, 6.50, 10.85)	m^3/m^3	[68]
	Vene flared gas volume	Triangle (0.66, 14.82, 28.98)	m^3/m^3	[68]
	Sirri flared gas volume	Triangle (37.10, 46.52, 55.94)	m^3/m^3	[68]
	Flaring efficiency[a]	PERT (80%, 95%, 99%)		[5,6,8,11,14]
	PG methane concentration[a]	Beta (14.49, 2.91, XBounds (0.989))	%mol	[11]
	Refinery yield factor	Triangle (190%, 100%, 110%)		[12]
	Distributed to bulk terminals[a]	Uniform (0, 1)		[5,13]

[a] From F-2 model in chapter 2 [16].

Table 13
Crude-specific Monte Carlo input distributions.

Arab Light	Production GOR	ModPERT (37.58, 98.85, 214.25, 15)	m^3/m^3	[24,42]
	Injection WOR	Triangle (1, 1.8, 5, WCopula)	m^3/m^3	[10,16,24]
	Production WOR	Triangle (0, 0.72, 5, WCopula)	m^3/m^3	[8,24]
	Water copula	CopulaBiFrank (10, 1)		
	Water injection pressure	Triangle (17.9, 20.7, 23.4)	MPa	[8,42]
	PG methane concentration	Triangle (36.7%, 44.3%, 54.4%)	%mol	[42]
	Petroline throughput	Triangle (4.29e5, 4.77e5, 5.25e5)	m^3/d	
Vene	Production GOR	Triangle (53.43, 97.96, 178.1)	m^3/m^3	[28,30]
	HS injection SOR	Triangle (1, 2.1, 5, WCopula)	m^3/m^3	[26,27,29]
	LS injection SOR	Triangle (0.01, 0.25, 0.7, WCopula)	m^3/m^3	[26,27,29]
	Production WOR	Triangle (0.3, 2, 3, WCopula)	m^3/m^3	[26]
	Water copula	CopulaBiFrank (10, 1)		
	Steam energy required	Triangle (1675, 1924, 2349)	kJ/kg	[16,27–29,40]
Sirri	Production GOR	Triangle (53.43, 133.58, 195.91)	m^3/m^3	[33,41,89]
	Injection WOR	Triangle (0.5, 2.7, 5.7, WCopula)	m^3/m^3	[33,41,90]
	Production WOR	Triangle (0.5, 1, 5.7, WCopula)	m^3/m^3	[33]
	Water copula	CopulaBiFrank (10, 1)		
	Water injection pressure	Triangle (17.9, 27.6, 31.0)	MPa	[33,41]
	Produced water treatment	Triangle (0.31, 0.63, 1.26)	kWh/m^3	[13,43,85,91]

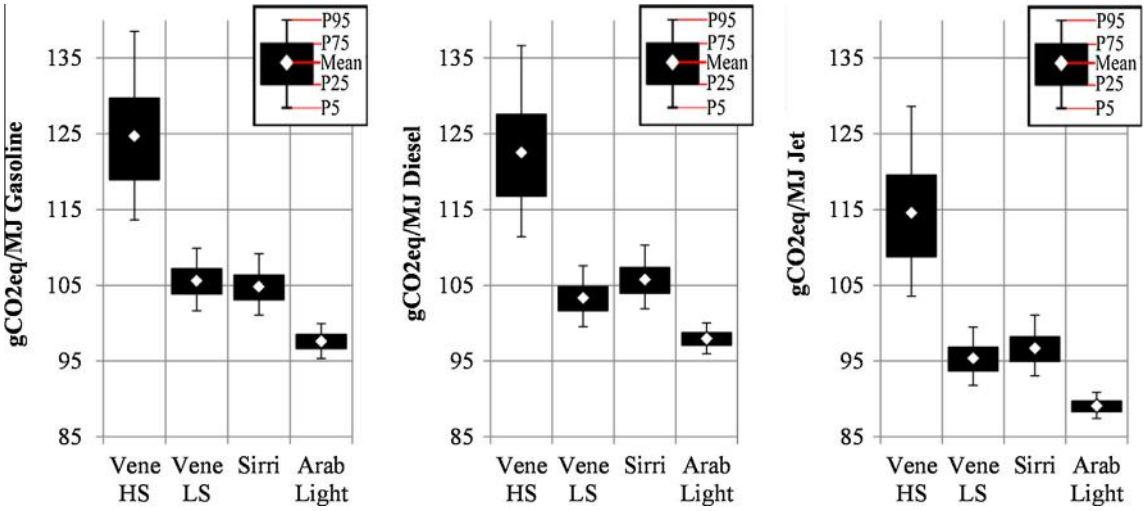

Fig. 4. Uncertainty in gasoline WTT + C emissions.

Vene HS scenario; there, the injection SOR had the largest effect. Hence a more detailed analysis of the refinery emissions is recommended to improve the model's accuracy, especially for the Arab Light scenario where the refinery emissions were the dominating source of uncertainty. For the Vene HS scenario, the injection SOR, steam energy required, and NG boiler efficiency are the dominating factors. This is expected as the WTT + C analysis showed that thermal extraction methods produce higher emissions due to the large amount of energy required. The marine diesel (MD) upstream EF had a significant effect due to the long transportation distances. The transportation emissions are small, but for the Arab Light scenario, where the WTT + C emissions are low, the transportation inputs have a measurable effect. Therefore, for low emission crudes a detailed analysis of the transportation emissions is required to further reduce uncertainty in WTT + C emissions. The tornado plots are not able to accurately represent dependent variables. In all scenarios, the production WOR and injection WOR/SOR are dependent; as a result, the production WOR appears to be more significant than it actually is.

4.3.2. Sources of uncertainty in VFF emissions

As Fig. 5 shows, the inputs related to the VFF emissions are a significant source of uncertainty. Further investigation shows that the uncertainty in the VFF emissions ranges from ±30% to ±55%, as shown in Fig. 6. For the Vene LS and Sirri scenarios, the VFF variances (P95-P5) are 5.8 and 7.1 gCO_2eq/MJ, while the WTT + C variances are 8.3 and 8.1 gCO_2eq/MJ, respectively. This means that a significant portion of the overall uncertainty is due to the VFF emissions. For Arab Light and Vene HS, the VFF uncertainty is not as significant with the VFF variance at 2.2 and 5.9 gCO_2eq/MJ, while the WTT + C variances are 4.6 and 24.9 gCO_2eq/MJ, respectively. For the Vene HS scenario, the injection SOR reduces the impact from the VFF emissions. For the Arab Light scenario, the overall low VFF emissions reduce their effect on WTT + C uncertainty.

Fig. 7 provides additional detail on which input has the largest effect on the VFF uncertainty. For the Vene scenarios, the production GOR and flaring and fugitive volumes have the largest effect due to their wide uncertainty ranges. For the Sirri scenario, the flaring efficiency and CH_4 global warming potential (GWP) are more significant due to the large flaring volumes seen in Iran. For the Arab Light scenario, the low methane concentration and flared volume reduces the significance of the flaring efficiency, flared gas volume, and CH_4 GWP.

4.3.3. Sources of uncertainty in refinery emissions

Fig. 8, shows that the natural gas upstream EF has the largest effect on refinery emissions uncertainty. Thus examining the

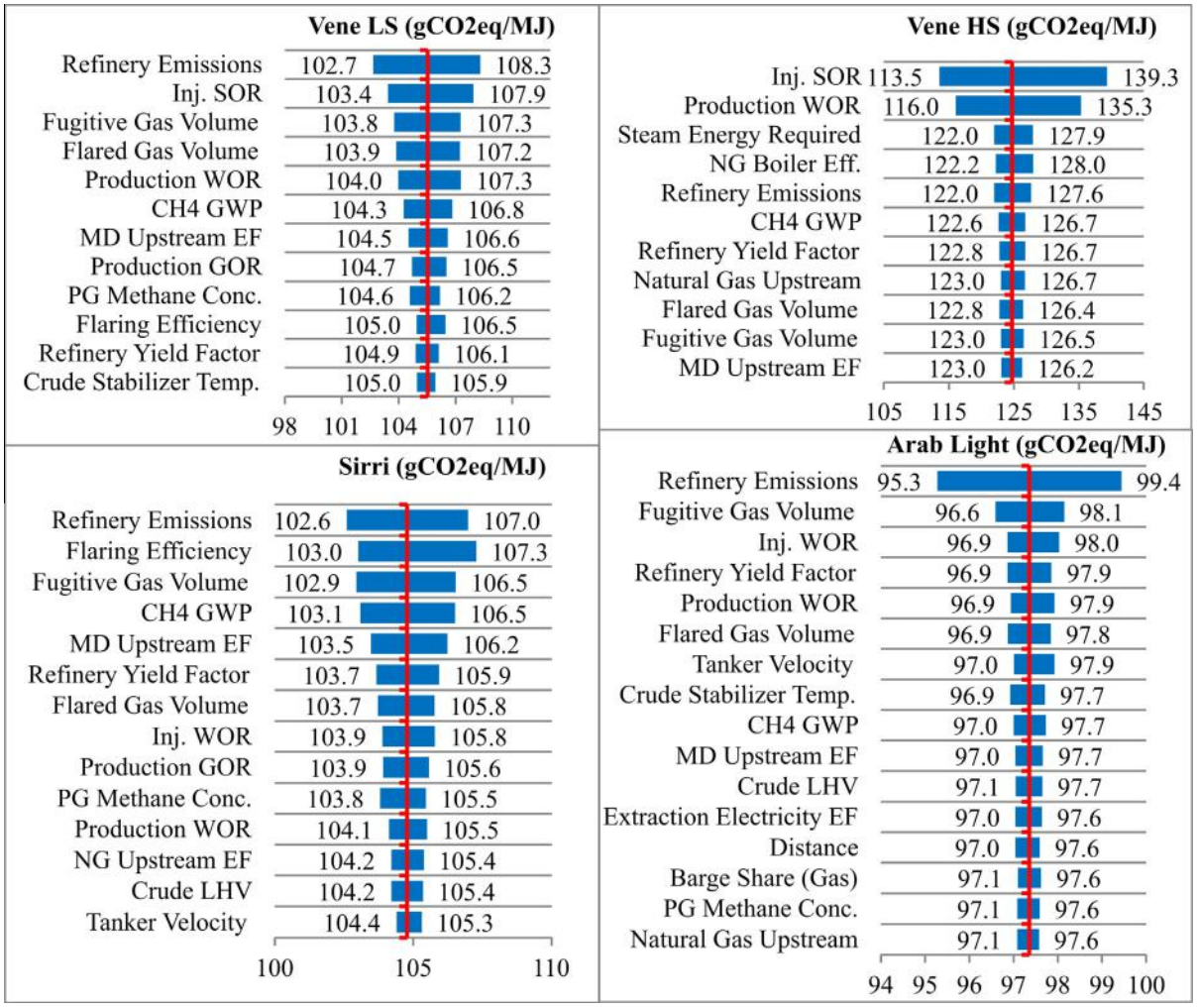

Fig. 5. Gasoline WTT + C tornado plots.

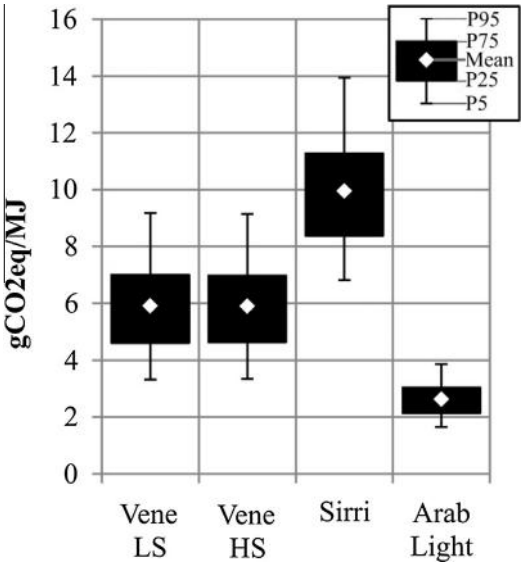

Fig. 6. Uncertainty in VFF emissions.

refinery's source of natural gas would improve estimates accuracy. The variation between the three scenarios is a result of the crude composition affecting flow rates to each process unit. For example, heavier crudes will have higher flow rates through the vacuum distillation tower.

5. Discussion

In this section, this study's results are compared with those in published literature. Then the F-2 and F-3 results are compared to show the differences in WTT + C emissions of North American and imported crudes (Fig. 9).

5.1. Comparison to published literature

Since this work uses a wide range of values for the inputs, the results from this study should encompass the results from previous studies if consistent boundaries are used. However, the boundaries are not consistent across all the models and hence the results vary. In order to verify that this study's results are nonetheless in agreement with those in the previous literature, the variation is explained.

Fig. 9 shows that the Jacobs North American results are within this study's uncertainty ranges [8]. For the Vene LS scenario, the Jacobs N.A. results are on the lower end of this study's distribution as Jacobs uses a production WOR of 0.25 and a production GOR of 16.0 m^3/m^3 compared to this studies 2.0 and 101.5 m^3/m^3. The low GOR used by Jacobs represents the field's original GOR while the current production GOR used here is from current wells. For the

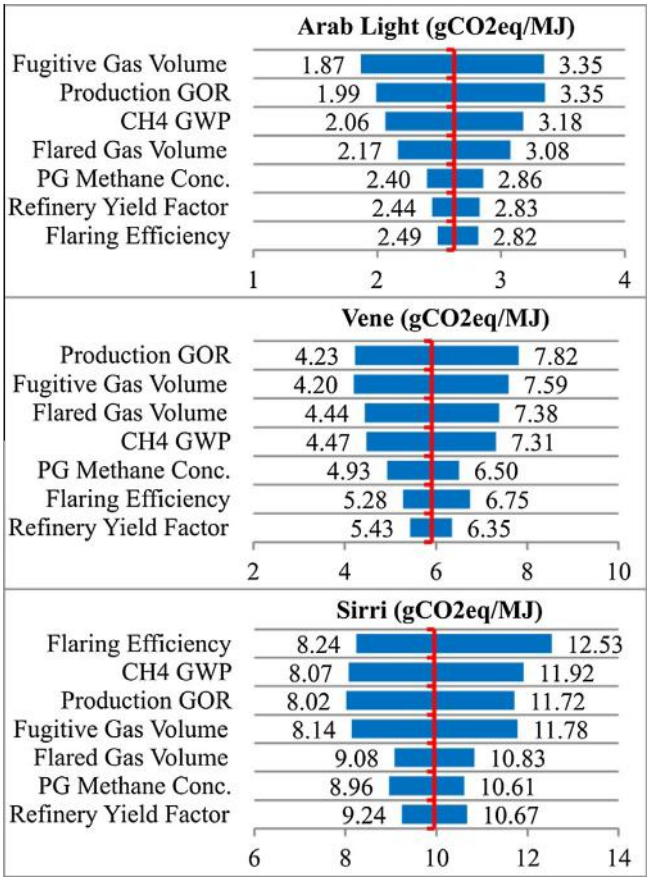

Fig. 7. VFF tornado plots.

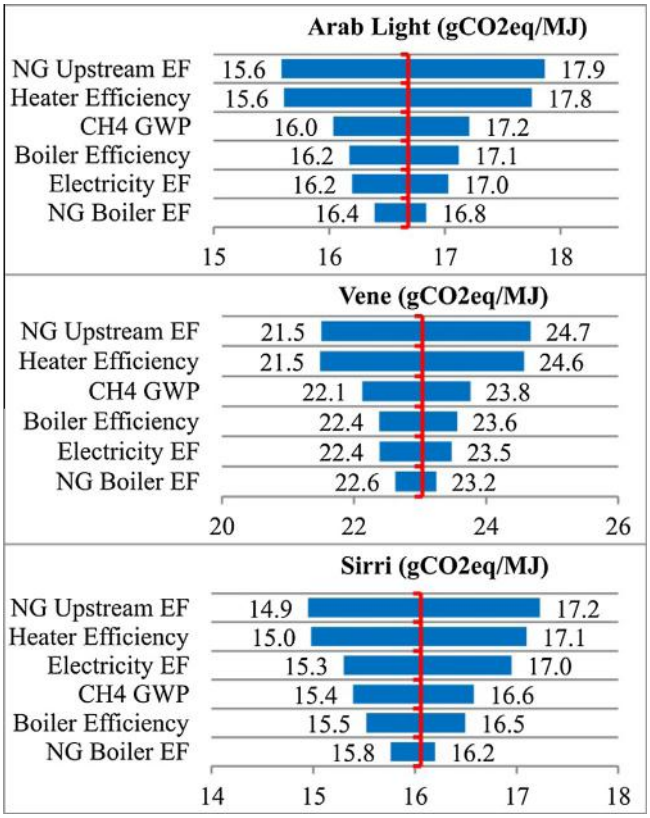

Fig. 8. Refinery tornado plots.

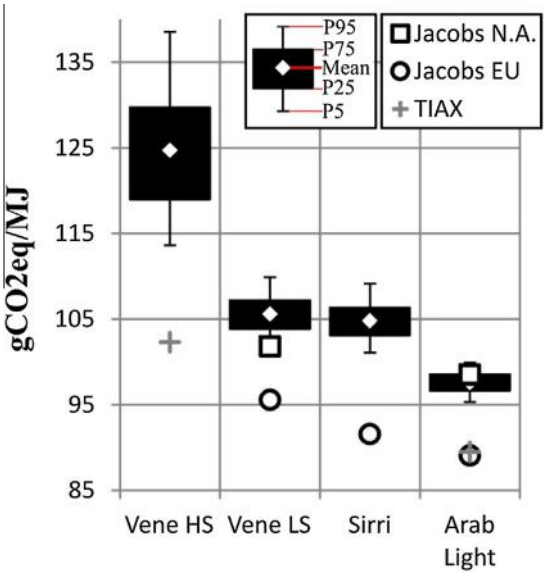

Fig. 9. WTT + C emissions comparison to previous literature.

Arab Light scenario, the Jacobs N.A. results use Arab medium oil. This study examined Arab Light due to data availability; as a result, the Jacobs emissions should be lower than our results. However, the Jacobs study used a higher injection WOR (2.3 vs. 1.8 m^3/m^3) and production GOR (115.8 vs. 101.5 m^3/m^3), which increased the emissions.

The Jacobs EU study assumed the crudes would be refined in Europe and use medium conversion refineries while this study and assumes deep conversion refineries, which have higher energy intensities [9]. As a result, the European results tend to be lower than the North American results, as seen from the Jacobs EU and N.A. results for the Arab Light scenario. For the Sirri scenario, the Jacobs EU refinery emissions are 7.4 gCO_2eq/MJ compared to this study's results of 16.1 gCO_2eq/MJ. As deep conversion refineries are the most GHG intensive refinery configuration, it makes sense that the Jacobs EU results are lower than this study's results.

TIAX performs a high level analysis that is not as detailed as the analyses done by Jacobs N.A. or this study. Therefore, its results are lower than results from Jacobs and this study [10]. The largest source of variation between TIAX and this study is in refinery and VFF emissions. The TIAX refinery emissions are 4.3 and 1.4 gCO_2eq/MJ lower than our results for the Vene and Arab Light scenarios and the VFF emissions are 4.1 and 2.4 gCO_2eq/MJ lower. The refinery variation is a result of the TIAX model using aggregated data from the United States to represent a typical refinery rather than using a deep conversion refinery. Overall, TIAX's limited scope and high level analysis resulted in lower estimates when compared to Jacobs and this study.

Comparing this study's results to the previous literature showed that the main source of variation between the modeled results was the refinery configuration. However, the variations caused by the assumed input values were included in this study's uncertainty ranges. This is important for policy makers as it shows this study's results give a fair representation of each crude's WTT + C emissions. Additionally, the use of input distributions reduces the F-3 model's sensitivity to author bias (unintentional or intentional).

5.2. Comparison to F-2 model results

To provide a better understanding of the uncertainty in the WTT + C emissions of various crudes, this study's results are compared to the F-2 model results for North American crudes from Di Lullo [16]. The purpose of this comparison is first to verify that the

results are reasonable; if two crudes have similar properties and extraction methods. Then their WTT + C emissions should be similar. Second, the combined results are analyzed to determine if it is possible to group crudes based on their WTT + C emissions. If the uncertainty ranges are too large, it will not be possible to confidently state if one crude has higher emissions than another.

The results from the F-2 model have been updated to ensure that the model boundaries are consistent with the new F-3 model; additional information is in Section S3 of the SI. In Fig. 10, the historical scenarios for Alaska North Slope (ANS) and Kern use lifetime averaged data for the injection and production ratios while the current scenarios use recent data to show how the WTT + C emissions change as the fields age. Table 14 provides a brief summary of the F-2 and F-3 crudes [16].

Vene HS and Kern current both use steam injection to extract heavy oil, but the Kern scenario has higher emissions due to the injection SOR used, 7.8 m^3/m^3 for Kern vs. 2.1 m^3/m^3 for Vene HS. Sirri, Arab Light, Bow River, and Mars all use water injection to maintain reservoir pressure. Bow River has the highest emissions as it is heavier crude and uses a higher injection WOR. The Sirri scenario has similar emissions to Bow, even though it is a lighter crude, due to its high injection pressure. Mars emissions are lower as it uses a lower injection WOR and has a lower flared gas volume. Arab Light has the lowest emissions due to its small VFF emissions and low energy intensity extraction. Overall there were no unexpected variations in the results.

The results in Fig. 10 allow the crudes to be separated into three general groups based on their WTT + C emissions. Group A contains the high emission crudes, ANS Current, Kern Current, and Vene HS. Group B contains medium emission crudes, Bow River, ANS Historical, Vene LS, Kern Historical, and Sirri. Group C contains the low emission crudes, Maya, Arab Light, and Mars. The uncertainty ranges show that it is not possible to confidently state if a crude has higher or lower emissions than another crude within its group. However, crudes in Group A have no overlap in their uncertainty ranges with Group B and C crudes. There is overlap between Group B's and C's 5th and 95th percentile ranges; however, there is no overlap between the 25th and 75th percentile ranges. To reduce the uncertainty ranges, either additional data are required or each crude should be further divided into specific extraction sites.

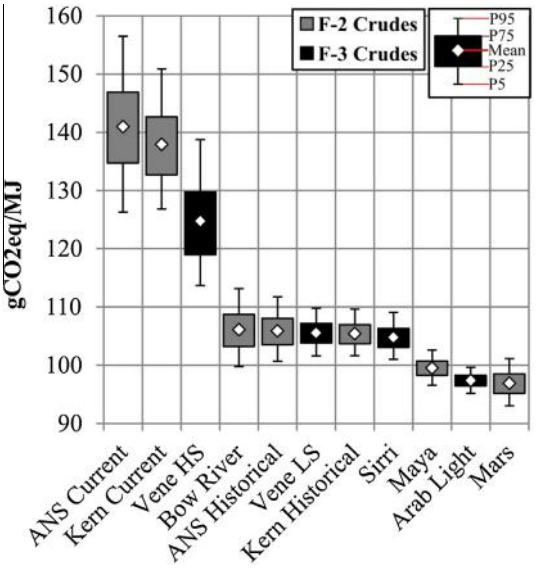

Fig. 10. Comparison of F-2 and F-3 gasoline WTT + C emissions.

6. Conclusion

The existing literature on the Well-to-tank + combustion (WTT + C) greenhouse gas (GHG) emissions of transportation fuels produced limited point estimates. This study used Monte Carlo simulations to quantify the uncertainty in the WTT + C emissions for three crudes from Saudi Arabia, Venezuela, and Iran. An updated version of the **FUN**damental E**N**gineering Princip**l**E**s**-based Mode**L** for Estimation of **G**reen**H**ouse **G**ases in **C**onventional **C**rude **O**ils (FUNNEL-GHG-CCO (FUNNEL-GHG-CCO) was used to perform a transparent WTT + C analysis for the three crudes previously studied by consulting companies.

The results showed that the Vene HS scenario clearly had the highest emissions at 113.6–138.5 gCO_2eq/MJ as its uncertainty range did not overlap with the remaining crudes. The Vene LS and Sirri scenarios had similar WTT + C emissions of 101.6–109.9 and 101.1–109.2 gCO_2eq/MJ, respectively. The Arab Light scenario uncertainty range did not overlap with any of the other crudes and had the lowest WTT + C emissions at 95.3–99.9 gCO_2eq/MJ.

The largest sources of uncertainty in WTT + C emissions were the VFF, refining, and injection SOR inputs. To reduce uncertainty in refining emissions, additional information from industry is required to develop an in-depth refinery model. Working with refinery operators the F-3 model could be used to minimize the WTT + C emissions from blends. To reduce uncertainty in VFF emissions, site-specific rather than aggregated country-wide data are required. VFF emissions require extensive on-site measurements as the current literature is limited. For example, flaring volume measurements use satellite images that have limited accuracy and do not differentiate between oil fields. For the Vene HS scenario, limited data availability for the injection SOR resulted in a wide conservative range being assumed; improved data availability could narrow this range.

The uncertainty ranges produced in this study will give policy makers and industry representatives a better understanding of the limits of bottom-up WTT + C models. Using a range of inputs will also give readers insight into how the assumed input values can affect the WTT + C emissions and also will give policy makers more confidence when using the numbers as they will not need to ask how emissions will change if input numbers change. Furthermore, this study's results are not as sensitive to author bias (intentional or unintentional) as they might be because the input

Table 14
Summary of F-2 and F-3 crudes.

Crude	°API	Extraction technology	Crude location	Refinery location
Maya	22.0	N_2 injection & gas lift	Mexico	Houston, TX
Mars	31.5	Water injection	U.S. Gulf Coast	Cushing, OK
Bow River	24.7	Water injection and pump lift	Canada	Cushing, OK
ANS	31.9	Water-alternating-gas injection	Alaska	Los Angeles, CA
Kern	13.0	Steam injection and pump lift	California	Los Angeles, CA
Vene	11.7	Steam injection	Venezuela	Houston, TX
Sirri	31.0	Water injection	Iran	Houston, TX
Arab Light	32.6	Water injection	Saudi Arabia	Houston, TX

ranges include a wide range of values taken from multiple sources. Additionally, the results of this study can be used to identify areas for potential GHG emission reductions and set realistic climate change policy targets.

Acknowledgements

The authors thank the NSERC/Cenovus/Alberta Innovates Associate Industrial Research Chair Program in Energy and Environmental Systems Engineering and the Cenovus Energy Endowed Chair Program in Environmental Engineering for funding the research project. We also thank representatives from Alberta Innovates – Energy and Environment Solutions (AI-EES), Alberta Innovates – Bio Solutions (AI-BIO), Cenovus Energy, and Suncor Energy for their inputs in various forms. The authors acknowledge the help of Dr. Abayomi Oni for his feedback related to refinery modeling. The authors are thankful to Astrid Blodgett for editorial assistance in this paper.

Appendix A. Supplementary material

Supplementary data associated with this article can be found, in the online version, at http://dx.doi.org/10.1016/j.apenergy.2016.10.027.

References

[1] The World Bank. Carbon Pricing: It's on the move. The World Bank; Nov. 30, 2015. <http://www.worldbank.org/en/news/feature/2015/11/30/carbon-pricing-its-on-the-move> [Apr. 12, 2016].
[2] California Air Resources Board. Low carbon fuel standard program background; Feb. 2, 2016. Available from: <http://www.arb.ca.gov/fuels/lcfs/lcfs-background.htm> [cited Feb. 11, 2016].
[3] The European Parliament and the Council of the European Union, Directive 2009/30/EC. Off J Europ Union, vol. 52; 2009. p. 88–113 [June 14, 2016], http://dx.doi.org/10.3000/17252555.L_2009.140.eng.
[4] Defining Life cycle Assessment [cited Apr. 14, 2016]; Available from: <http://www.gdrc.org/uem/lca/lca-define.html>.
[5] Argonne. GREET1. Argonne, IL: Argonne National Laboratory; 2015, <https://greet.es.anl.gov/> [June 14, 2016].
[6] (S&T)^2 Consultants Inc. GHGenius. Delta, BC: (S&T)^2 Consultants Inc; 2012, <http://www.ghgenius.ca/downloads.php> [May 16, 2016].
[7] Orsi F et al. A multi-dimensional well-to-wheels analysis of passenger vehicles in different regions: primary energy consumption, CO_2 emissions, and economic cost. Appl Energy 2016;169:197–209. doi: http://dx.doi.org/10.1016/j.apenergy.2016.02.039.
[8] Keesom W, Unnasch S, Moretta J. Life cycle assessment comparison of North American and imported crudes prepared for Alberta energy research institute. Chicago, IL: Jacobs Consultancy; July 2009, <http://eipa.alberta.ca/media/39640/life%20cycle%20analysis%20jacobs%20final%20report.pdf> [June, 14, 2016].
[9] Keesom B, Blieszner J, Unnasch S. EU pathway study: life cycle assessment of crude oils in a European context. Chicago, IL: Jacobs Consultancy; Mar. 2012, <http://www.energy.alberta.ca/Oil/pdfs/OSPathwayStudyEUjacobsRept2012.pdf> [June 14, 2016].
[10] Rosenfeld J et al. Comparison of North American and imported crude oil lifecycle GHG emissions – final report prepared for Alberta Energy Research Institute. Cupertino, CA: TIAX LLC; July 6, 2009, <http://eipa.alberta.ca/media/39643/life%20cycle%20analysis%20tiax%20final%20report.pdf> [Mar. 25, 2016].
[11] El-Houjeiri HM, et al., OPGEE. Stanford, CA: Stanford School of Earth, Energy & Environmental Sciences; June 4, 2015. <https://pangea.stanford.edu/researchgroups/eao/research/opgee-oil-production-greenhouse-gas-emissions-estimator> [May 16, 2016].
[12] Bergerson J. Petroleum refinery life cycle inventory model. Calgary, AB: University of Calgary; 2015, http://ucalgary.ca/lcaost/prelim [May 16, 2016].
[13] Rahman MM. Life cycle assessment of North American Conventional crudes for production of transportation fuels. In: Mechanical engineering. Edmonton: University of Alberta; 2014.
[14] Rahman MM, Canter C, Kumar A. Greenhouse gas emissions from recovery of various North American conventional crudes. Energy 2014;74:607–17. doi: http://dx.doi.org/10.1016/j.energy.2014.07.026 [June 14, 2016].
[15] Rahman MM, Canter C, Kumar A. Well-to-wheel life cycle assessment of transportation fuels derived from different North American conventional crudes. Appl Energy 2015;156:159–73. doi: http://dx.doi.org/10.1016/j.apenergy.2015.07.004 [June 14, 2016].
[16] Di Lullo GR. Uncertainty in life cycle assessments of well-to-wheel greenhouse gas emissions of transportation fuels derived from various crude oils. In: Mechanical engineering. Edmonton, AB: University of Alberta; 2016.
[17] Gordon D et al. Know your oil: creating a global oil-climate index. Washington: Carnegie Endowment for International Peace; 2015, <http://carnegieendowment.org/files/know_your_oil.pdf> [Feb. 18, 2016].
[18] US Energy Information Administration. Weekly preliminary crude imports by top 10 countries of origin (ranking based on 2013 Petroleum Supply Monthly data). Washington: EIA; 2016. June 6.
[19] Asghedom A. Iran's petroleum production expected to increase as sanctions are lifted. Washington: U.S. Energy Information Administration; 2016. Jan. 19.
[20] Vose Software. ModelRisk Software. Belgium: Vose Software; 2015, <http://www.vosesoftware.com/> [May 16, 2016].
[21] API gravity; May 8, 2016. Available from: <https://en.wikipedia.org/wiki/API_gravity> [cited June 14, 2016].
[22] Al-Mutairi SM, Al-Harbi M. Water production management strategy in North Uthmaniyah area, Saudi Arabia. In: Europec/EAGE annual conference and exhibition. Vienna: Society of Petroleum Engineers; 2006 [June 14, 2016].
[23] Simmons MR. Twilight in the desert: the coming Saudi oil shock and the world economy. Hoboken, New Jersey: Wiley; 2005.
[24] Alhuthali AHH et al. Water management in North 'Ain Dar, Saudi Arabia. In: 14th Middle east oil & gas show and conference. Bahrain: Society of Petroleum Engineers; 2005 [June 15, 2016].
[25] Al-Ahmed A, Bond A, Morillo D. Security threats to Saudi Arabia's oil infrastructure. Washington: The Institute for Gulf Affairs; 2013, <http://www.gulfinstitute.org/wp-content/uploads/2013/11/Threats_to_the_Saudi_Oil_Infrastructure.pdf> [Apr. 4, 2016].
[26] Chourio Arocha GJ, Mohtadi M, Ortega JB. Evaluation and application of the extended cyclic steam injection as a new concept for Bachaquero-01 reservoir in west Venezuela. In: SPE reservoir characterisation and simulation conference and exhibition. Abu Dhabi, UAE: Society of Petroleum Engineers; 2011 [June 14, 2016].
[27] Rodriguez MG, Mamora DD. Increased oil production from Bachaquero-01 by steamflooding using horizontal wells. In: SPE/DOE improved oil recovery symposium. Tulsa, Oklahoma: Society of Petroleum Engineers; 2000 [June 14, 2016].
[28] Rodriguez MG. Bachaquero-01 Reservoir, Venezuela—increasing oil production by switching from cyclic steam injection to steamflooding using horizontal wells. Texas: Texas A&M University; 1999.
[29] Escobar MA, Valera CA, Perez RE. A large heavy oil reservoir in Lake Maracaibo Basin: cyclic steam injection experiences. In: International thermal operations and heavy oil symposium. Bakersfield, California: Society of Petroleum Engineers; 1997 [June 14, 2016].
[30] Potma J et al. Thermal horizontal completions boost heavy oil production. World Oil 2003;224(2):83–5, <http://www.worldoil.com/magazine/2003/february-2003/features/thermal-horizontal-completions-boost-heavy-oil-production> [June 14, 2016].
[31] Oil and Gas Journal. Total seeks to replicate its Sirri development success off Iran. Oil Gas J 1999;97(14). <http://www.ogj.com/articles/print/volume-97/issue-14/in-this-issue/drilling/total-seeks-to-replicate-its-sirri-development-success-off-iran.html> [Apr. 12, 2016].
[32] A Barrel Full. Sirri Island Oil Fields. 2015 June 29; 2015; Available from: <http://abarrelfull.wikidot.com/sirri-island-oil-fields> [cited Apr. 12, 2016].
[33] Taheri A et al. Simulation and experimental studies of mineral scale formation effects on performance of Sirri-C oil field under water injection. Iran J Chem Chem Eng 2011;30(3):9–24, <http://www.sid.ir/en/vewssid/j_pdf/84320115902.pdf> [June 14, 2016].
[34] Maroos Shipping and Forwarding Co. Sirri Island; 2016. Available from: <http://www.maroos.net/page/siri-island.html> [cited Apr. 12, 2016].
[35] Nimana B, Canter C, Kumar A. Energy consumption and greenhouse gas emissions in the recovery and extraction of crude bitumen from Canada's oil sands. Appl Energy 2015;143:189–99. doi: http://dx.doi.org/10.1016/j.apenergy.2015.01.024 [June 28, 2016].
[36] El-Houjeiri HM, et al., OPGEE V1.1 Draft D: User guide & Technical documentation. Stanford, CA: Stanford School of Earth, Energy & Environmental Sciences; Oct. 10, 2014. <https://pangea.stanford.edu/researchgroups/eao/research/opgee-oil-production-greenhouse-gas-emissions-estimator> [June 14, 2016].
[37] Yeh S et al. Land use greenhouse gas emissions from conventional oil production and oil sands. Environ Sci Technol 2010;44(22):8766–72. doi: http://dx.doi.org/10.1021/es1013278 [June 14, 2016].
[38] Sorkhabi R. The king of giant fields. In: GEO ExPro; 2010. p. 24–29.
[39] Saleri NG, Bu-Hulaigah EH. Knowledge managment in North Ghawar. In: 17th World Petroleum congress. Rio de Janeiro, Brazil: World Petroleum Congress; 2002, <https://www.onepetro.org/conference-paper/WPC-32150> [June 15, 2016].
[40] Çengel Y, Boles MA. Thermodynamics: an engineering approach. 7th ed. New York: McGraw-Hill; 2011.
[41] Taheri A et al. Evaluation of reservoir performance under water injection considering the effect of inorganic scale deposition in an Iranian carbonate oil reservoir. In: 8th European formation damage conference. Scheveningen, Netherlands: Society of Petroleum Engineers; 2009 [June 14, 2016].
[42] Al-Eid MI, Kokal SL. Investigation of increased gas-oil ratios in Ain Dar field. In: 13th Middle east oil show & conference. Bahrain: Society of Petroleum Engineers; 2003 [June 14, 2016].

[43] Samandis Company. Project: Sirri district Industrial Wastewater Treatment system EPC Project. Available from: <http://samandis-co.com/2-3.html> [cited Apr. 12, 2016].

[44] Canter C, Kumar A. Impact of fugitive emissions on the greenhouse gas emissions of conventional crudes. In: AIChE annual meeting. Atlanta: AIChE; 2014.

[45] US Energy Information Administration. PAD district imports by country of origin. Washington: EIA; 2016 [May 5].

[46] Soligo R, Jaffe AM. Unlocking the assets: energy and the future of central Asia and the caucasus. In: The economics of pipeline routes: the conundrum of oil exports from the Caspin basin. Houston, Texas: The James A. Baker III Institute for Public Policy of Rice University; Apr. 1998, <http://bakerinstitute.org/files/2753/> [May 4, 2016].

[47] Enbridge Pipelines Inc. Q2 2015 Service Levels On the Enbridge Liquids Pipeline Mainline Network. Calgary, AB: Enbridge; June 2015, <http://www.enbridge.com/~/media/Rebrand/Documents/Shippers/Enbridge_Mainline_Service_Levels.pdf?la=en> [June 14, 2016].

[48] Karassik IJ et al. 2.1 Centrifugal pump theory. In: Pump Handbook. New York: McGraw Hill Professional; 2015, <http://accessengineeringlibrary.com/browse/pump-handbook-fourth-edition> [January 26, 2016].

[49] (S&T)^2 Consultants Inc., Shale Gas Update for GHGenius. Ottowa: Natural Resources Canada Office of Energy Efficiency; Aug. 31, 2011. <http://www.ghgenius.ca/reports/ShaleGasUpdateFinalReport.pdf> [June 14, 2016].

[50] Oil and Gas Journal. Crude Oil Assays. In: Oil and Gas Journal DataBook 2008. Tulsa, OK: PennWell Books; 2008. p. 231, <https://books.google.ca/books?id=Vb9VAgAAQBAJ>.

[51] Stratiev D et al. Evaluation of crude oil quality. Pet Coal 2010;52(1):35–43, <http://www.vurup.sk/sites/vurup.sk/archivedsite/www.vurup.sk/pc/vol52_2010/issue1/pdf/pc_1_2010_stratiev_051.pdf> [June 14, 2016].

[52] Enviroment Canada. Arabian Light. Ottawa: Emergencies Science and Technology Division; 1991.

[53] Sea Distance Calculator. Available from: <http://www.sea-distances.org/> [cited Apr. 28, 2016].

[54] Hamilton TM. Oil tanker sizes range from general purpose to ultra-large crude carriers on AFRA scale. In: Today in energy. U.S. Energy Information Administration; 2014.

[55] Saudi Arabia: Hydrocarbon Sector Transport and Storage Facilities. 1992 Dec.; 1992. Available from: <http://www.country-data.com/cgi-bin/query/r-11616.html> [cited May 4, 2016].

[56] Cerić E. Crude oil assay. Emir Ceric; 2001.

[57] Weber CL, Clavin C. Life cycle carbon footprint of shale gas: review of evidence and implications. Environ Sci Technol 2012;46(11):5688–95. doi: http://dx.doi.org/10.1021/es300375n [June 14, 2016].

[58] U.S. Energy Information Administration. Country analysis brief: Venezuela. Washington: EIA; 2015. Nov. 25.

[59] Venezuela: Electricity Sector Statistics. Available from: <http://mecometer.com/infographic/venezuela/electricity-sector-statistics/> [cited May 4, 2016].

[60] Deputy for Power & Energy Affairs Power & Energy Planning Department. Iran and world energy facts and figures, 2012. Iran: Ministry of Energy; 2012.

[61] Trading Economics. Electricity production from oil sources (% of total) in Saudi Arabia. New York; 2016. Available from: <http://www.tradingeconomics.com/saudi-arabia/electricity-production-from-oil-sources-percent-of-total-wb-data.html> [cited Apr. 4, 2016].

[62] Segar C. Saudi energy mix: renewables augment gas. IEA Energy: J Int Energy Agency 2014(7):40, <http://www.iea.org/ieaenergy/issue7/saudi-energy-mix-renewables-augment-gas.html> [June 14, 2016].

[63] Publications IB. Middle East Countries Mineral Industry Handbook. Strategic information and regulations, vol. 1. Washington: LuLu Press; 2015.

[64] Enviromental Protection Agency. eGRID Data Files. Washington, DC: Energy and the Environment; 2016. Jan. 4.

[65] van Hauwermeiren M, Vose D. A compendium on distributions. Ghent, Belgium: Vose Software; 2009.

[66] van Hauwermeiren M, Vose D. A compendium on distributions. Ghent, Belgium: Vose Software; 2009, <http://www.vosesoftware.com/content/ebookmr4.pdf> [March 14, 2016].

[67] Aspen Technology Inc. Aspen HYSYS Refiney Wide Model.hsc, <http://www.aspentech.com/products/aspen-hysys/>; 2016 [May 16, 2016].

[68] National Oceanic and Atmospheric Administration. Global/Country Results 1994–2010. Washington: NOAA; 2011. Feb. 23.

[69] Myhre G et al. Anthropogenic and natural radiative forcing supplementary material. In: Stocker TF et al., editors. Climate change 2013: the physical science basis. Contribution of working group to the fifth assessment report of the intergovernmental panel on climate change. Cambridge and New York: Cambridge University Press; 2013. p. 8SM-19 <https://www.ipcc.ch/pdf/assessment-report/ar5/wg1/supplementary/WG1AR5_Ch08SM_FINAL.pdf>.

[70] Myhre G et al. Anthropogenic and natural radiative forcing. In: Stocker TF et al., editors. Climate change 2013: the physical science basis. Contribution of working group to the fifth assessment report of the intergovernmental panel on climate change. Cambridge and New York: Cambridge University Press; 2013.

[71] U.S. Energy Information Administration. Natural gas gross withdrawals and production. Washington: U.S. EIA; 2015. July 31.

[72] Cleaver Brooks. Boiler efficiency guide: facts about firetube boilers and boiler efficiency, Mar. 2010. Thomasville, GA: Cleaver Brooks; 2010, <http://www.cleaver-brooks.com/reference-center/insights/boiler-efficiency-guide.aspx> [June 14, 2016].

[73] Stark C. Reducing energy cost through boiler efficiency. Raleigh, NC: Department of Poultry Science North Carolina State University; 2015, <https://www.ncsu.edu/project/feedmill/pdf/E_Reducing%20Energy%20Cost%20Through%20Boiler%20Efficiency.pdf> [Mar. 25, 2016].

[74] Energy Technology Systems Analysis Program. Industrial combustion boilers. In: IEA ETSAP - Technology Brief I01, May 2010. Paris, FR: International Energy Agency; 2010, <http://www.iea-etsap.org/web/e-techds/pdf/i01-ind_boilers-gs-ad-gct1.pdf> [June 14, 2016].

[75] Council of Industrial Boiler Owners. Energy efficiency & industrial boiler efficiency: an industry perspective. Warrenton, VA: Council of Industrial Boiler Owners; 2015, <http://www.swagelokenergy.com/download/EEIBE.pdf> [Feb. 18, 2016].

[76] Devco Process Heaters. *Our Heaters*. Available from: <http://www.devcoheaters.com/our-heaters/> [cited Feb. 16, 2016].

[77] Wildy F. Fired heater optimization. Pittsburgh, PA: AMETEK Process Instruments; 2016, <http://www.etaassociates.com/Fired%20Heater%20Optimization%20ISA%20AD.pdf> [Mar. 25, 2016].

[78] Evans J. Centrifugal pump efficiency—what is efficiency? In: Pumps & systems. Birmingham, AL: Pumps & Systems; 2012, <http://www.pumpsandsystems.com/topics/pumps/pumps/centrifugal-pump-efficiency-what-efficiency> [March 30, 2016].

[79] Campell JM. Gas conditioning and processing. The equipment modules, vol. 2. Norman, OK: Campell Petroleum Series; 1984.

[80] Flowserve. Pipeline transportation pumps, Jan. 2015. Irving, TX: Flowserve; 2015, p. Brochure <http://www.flowserve.com/files/Files/Literature/ProductLiterature/Pumps/fpd-8-e.pdf> [May 16, 2016].

[81] Nesbitt B. Flow of liquids. In: Handbook of pumps and pumping: pumping manual international. Oxford, U.K.: Elsevier Science; 2006. p. 95–124.

[82] Wright W. Simple equations to approximate changes to the properties of crude oil with changing temperature, Apr. 1. Norman, OK: John M. Campbell Consulting; 2014, <http://www.jmcampbell.com/tip-of-the-month/2014/04/simple-equations-to-approximate-changes-to-the-properties-of-crude-oil-with-changing-temperature/> [Feb. 17, 2016].

[83] Manning FS, Thompson RE. Oilfield processing of petroleum: crude oil, vol. 2. Tulsa, OK: PennWell Books; 1995.

[84] Stewart M, Arnold K. Chapter 2 - Crude stabilization, in emulsions and oil treating equipment. Burlington: Gulf Professional Publishing; 2009. p. 81–106.

[85] Vlasopoulos N et al. Life cycle assessment of wastewater treatment technologies treating petroleum process waters. Sci Total Environ 2006;367(1):58–70. doi: http://dx.doi.org/10.1016/j.scitotenv.2006.03.007 [June 14, 2016].

[86] Psaraftis HN, Kontovas CA. Ship emission study prepared for Hellenic Chamber of shipping, May 2008. Pireas, Greece: National Technical University of Athens Laboratory for Maritime Transport; 2008, <http://www.nee.gr/downloads/66ship.emissions.study.pdf> [June 14, 2016].

[87] Man Diesel & Turbo. Basic principles of ship propulsion, Dec. 2011. MAN Diesel & Turbo: Copenhagen, Denmark, <https://marine.man.eu/docs/librariesprovider6/propeller-aftship/basic-principles-of-propulsion.pdf?sfvrsn=0> [June 14, 2016].

[88] Lindstad H, Asbjørnslett BE, Strømman AH. Reductions in greenhouse gas emissions and cost by shipping at lower speeds. Energy Policy 2011;39(6):3456–64. doi: http://dx.doi.org/10.1016/j.enpol.2011.03.044 [June 14, 2016].

[89] Jafari M et al. Experimental study and simulation of different EOR techniques in a non-fractured carbonate core from an Iranian offshore oil reservoir. Iran J Chem Chem Eng 2008;27(2):81–91, <http://www.sid.ir/en/vewssid/j_pdf/84320080209.pdf> [June 14, 2016].

[90] Ashoori S et al. Efficiency improvement of sea water injection plant-experience from an offshore oil field. In: 20th World Petroleum Congress. 2011. Doha, Qatar: World Petroleum Congress, <https://www.onepetro.org/conference-paper/WPC-20-1151?sort=&start=0&q=Efficiency+Improvement+of+Sea+Water+Injection+PlantExperience+from+an+Offshore+Oil+Field&from_year=&peer_reviewed=&published_between=&fromSearchResults=true&to_year=&rows=10#> [June 14, 2016].

[91] VertMarkets Inc. OPUS® II Technology - a new innovation for produced water and Frac Flowback treatment [cited Apr. 12, 2016]; Available from: <http://www.oilandgasonline.com/doc/cophase-cfu-compact-flotation-unit-0001>; 2016.